Modeling of Offshore Wind and Tidal Current Turbines for Stability Analysis

Hamed H. H. Aly and M. E. El-Hawary

***Abstract*— Offshore wind and tidal current are of the most common energy resources for generating electricity in the near future because of the oil problems (crises and pollution). The dynamic model of the offshore wind and tidal current is very important topic for dealing with these renewable energies. This paper describes the overall dynamic models of offshore wind and tidal current turbine using three different types of generators (doubly fed induction generator (DFIG), squirrel cage induction generator (SCIG) and direct drive permanent magnet synchronous generator (DDPMSG)). The state space for all types of the generators are concluded. All models are validated using a common property of the generator for the validation.**

***Index Terms*— Offshore wind, Tidal current, Direct drive permanent magnet synchronous generator (DDPMSG), Doubly fed induction generator (DFIG).**

NOMENCLATURE

V_{tide}	Tidal current speeds.
V_{nt}	Neap tide speed.
V_{st}	Spring tide speed.
P_{ts}	Tidal in-stream power.
ρ	Density of the water (1025 kg/m^3)
A	Cross-sectional area perpendicular to the flow direction.
T_m	Mechanical torque applied to the turbine.
A	Cross-sectional area perpendicular to the flow direction.
C_p	Marine turbine blade design constant in the range of 0.35-0.5.
ω_s ,ω_r , ω_t	Stator, rotor electrical angular velocities, and turbine speed at hub height upstream the rotor.
T_e	Electrical torque of the generator.
D_s	Shaft stiffness damping.
H_t ,H_a	Turbine and generator inertia constants.
K_s	Shaft stiffness coefficient.
Θ_t ,Θ_r	Turbine and generator rotor angles.
β	Tidal turbine pitch angle.
S	Rotor slip.
d, q	Indices for the direct and quadrature axis components.
s, r	Indices of the stator and the rotor.
v, R, i, ψ	Voltage, resistance, current, and flux linkage of the generator.
K_{pt}, K_{it}	Coefficients for the proportional-integral controller of the pitch controller.
P_g, P_{DC}	Active power of the AC terminal at the grid side converter and DC link power respectively.
v_{Dg} , v_{Qg}	D and Q axis voltages of the grid side converter.
i_{Dg} ,i_{Qg}	D and Q axis currents of the grid side converter.
C	Capacitance of the capacitor.
v_{DC} , i_{DC}	Voltage and current of the capacitor.
K_{p1}, K_{p2}, K_{p3}	Proportional controller constants for the generator side converter controller
K_{i1}, K_{i2} ,K_{i3}	Integral controller constants for the generator side converter controller.
i_{Dq}, i_{Qq}	D and Q axis grid currents.
v_{Da}, v_{Oa}	D and Q axis grid voltages.
K_{p4}, K_{p5}, K_{p6}	Proportional controller constants for the grid side converter.
K_{i4}, K_{i5}, K_{i6}	Integral controller constants for the grid side converter.
X_c	Grid side smoothing reactance.
$\dot{x}$	State variable

Manuscript received June 21, 2013; revised July 13, 2013. This work was supported in part by the Egyptian Governoment and Dalhousie University.

Hamed H. H. Aly was with Zagazig University, Zagazig, Egypt. He is now with the Department of Electrical & Computer Engineering at Dalhousie University, NS, B3H 4R2, Canada. (e-mail: hamed.aly@dal.ca).

M. E. El-Hawary is a professor at the Department of Electrical and Computer Engineering, Dalhousie University, Halifax, NS, B3H 4R2, Canada (e-mail: elhawary@dal.ca).

I. INTRODUCTION

Wind is hardly predictable source of energy. Tidal current turbines extract electric energy from the water. Tidal currents are fluctuating, intermittent but a predictable source of energy compared to wind. Its use is very effective as it relies on the same technologies used in wind turbines. The electrical-side layout and modeling approaches used in tidal in-stream systems are similar to those used for wind and offshore wind systems. The speed of water currents is lower than wind speed, while the water density is higher than the air density and as a result wind turbines operate at higher rotational speeds and lower torque than tidal in-stream turbines which operate at lower rotational speed and high torque [1-5].

The easier predictability of the tidal in-stream energy resource makes it easier to integrate in an electric power grid. Recognizing that future ocean energy resources are available far from load centers and in areas with limited grid capacity will result in challenges and technical limitations. With the growing penetration of tidal current energy into the electric power grid system, it is very important to study the impact of tidal current turbines on the stability of the power system grid and to do that we should model the overall

ISBN: 978-988-19252-3-7
ISSN: 2078-0958 (Print); ISSN: 2078-0966 (Online)

system. The model of the ocean energy system consists of three stages. The first stage contains the fluid mechanical process. The second stage consists of the mechanical conversion and depends on the relative motion between bodies. This motion may be mechanical transmission and then using mechanical gears or may be depending on the hydraulic pumps and hydraulic motors. The third stage consists of the electromechanical conversion to the electrical grid [4-9].

II. Offshore Wind and Tidal Current Model using IG

A. The Speed Signal Resource Model for the Tidal Current and Offshore Wind

The tidal current speed may be expressed as a function of the spring tide speed, neap tide speed and tides coefficient. Paper (10) proposed different algorithm models for the tidal current speed.

The Wind Speed Signals Model (v_w) consists of four components related to the mean wind speed (v_{mw}), the wind speed ramp (v_{rw}) (which is considered as the steady increase in the mean wind speed), the wind speed gust (v_{gw}), and the turbulence (v_{tw}). $v_w = v_{mw} + v_{gw} + v_{rw} + v_{tw}$

The mean wind speed is a constant; a simple ramp function will be used for ramp component (characterized by the amplitude of the wind speed ramp (A_r (m/s)), the starting time (T_{sr}), and the ending time (T_{er})). The wind speed gust component is characterized by the amplitude of the wind speed gust (A_g (m/s)), the starting time (T_{sg}), and the ending time (T_{eg}). The wind speed gust may be expressed as a sinusoidal function. The most used models are given by:

$v_{gw} = A_g(1-\cos(2\Pi(t/D_g - T_{sg}/D_g)))$ $\quad T_{sg} \le t \le T_{eg}$

$v_{gw} = 0$ $\quad t < T_{sg}$ or $t > T_{eg}$

$D_g = T_{eg} - T_{sg}$

A triangular wave is used to represent the turbulence function which has adjustable frequency and amplitude [11].

B. The Rotor Model

For the offshore wind the rotor model represents the conversion of kinetic energy to mechanical energy. The wind turbine is characterized by C_p (wind power coefficient), λ (tip speed ratio), and β (pitch angle). $\lambda = \omega_t R/v_w$, where R is the blade length in m, v_w is the wind speed in m/s, and ω_t is the wind turbine rotational speed in rad/sec. C_p-λ-β curves are manufacturer-dependent but there is an approximate relation expressed as

$$C_p = \frac{1}{2}\left(\frac{RC_f}{\lambda} - 0.026\,\beta - 2\right)e^{-0.295\frac{RC_f}{\lambda}},$$

C_f is the wind turbine blade design constant. The rotor model may be represented by using the equation of the power extracted from the wind ($P_w = 0.5\rho\Pi R^2 C_p v_w^3$) [11].

For the tidal current turbines the rotor model may be represented by using the equation of the power extracted from the wind ($P_w = 0.5\rho\Pi R^2 C_p v_w^3$),

The power (P_{ts}) may be found using: $P_{ts} = ½\ \rho A(V_{tide})^3$. The turbine harnesses a fraction of this power, hence the power output may be expressed as: $P_t = ½\ \rho C_p A(V_{tide})^3$. The power output is proportional to the cube of the velocity. The velocity at the bottom of the channel is lower than at the water column above seabed. The mechanical torque applied to the turbine (T_m) can be expressed as [4-9]:

$$T_m = \frac{0.5\rho\Pi R^2 C_p v_{tide}^3}{\omega_t} \quad (1)$$

The shaft system for tidal current and offshore turbines may be represented by a two mass system one for the turbine and the other for the generator as shown:

$$2H_t\frac{d\omega_t}{dt} = T_t - K_s(\Theta_r - \Theta_t) - D_s(\omega_r - \omega_t) \quad (2)$$

$$2H_g\frac{d\omega_r}{dt} = T_e - K_s(\Theta_r - \Theta_t) - D_s(\omega_r - \omega_t) \quad (3)$$

$$\Theta_{tr} = \Theta_r - \Theta_t \quad (4)$$

$$\frac{d\Theta tr}{dt} = \omega_r - \omega_t \quad (5)$$

There is a ratio for the torsion angles, damping and stiffness that need to be considered when one adds a gear box as all above calculations must be referred to the generator side and calculated as : $a=\frac{\omega_r}{\omega_t}$, $\omega_r^{(t)} = \frac{\omega_r^{(g)}}{a}$, $_t^{(t)} = \frac{_t^{(g)}}{a}$, $K_s^{(t)} = a^2 K_s^{(g)}$, $D_m^{(t)} = a^2 D_m^{(g)}$. The same model used for the offshore wind is used for tidal in-stream turbines; however, there is a number of differences in the design and operation of marine turbines due to the changes in force loadings, immersion depth, and different stall characteristics.

C. Dynamic Model of DFIG

The DFIG model is developed using a synchronously rotating d-q reference frame with the direct-axis oriented along the stator flux position. The reference frame rotates at the same speed as the stator voltage. The stator and rotor active and reactive power are given by [4-10]:

$$P_s = 3/2(v_{ds}\ i_{ds} + v_{qs}\ i_{qs}) \quad , \quad P_r = 3/2(v_{dr}\ i_{dr} + v_{qr}\ i_{qr}) \quad (6)$$

$$P_g = P_s + P_r \quad (7)$$

$$Q_s = 3/2(v_{qs}\ i_{ds} - v_{ds}\ i_{qs}) \quad , \quad Q_r = 3/2(v_{qr}\ i_{dr} - v_{dr}\ i_{qr}) \quad (8)$$

The model of the DFIG can be described as:

$$v_{ds} = -R_s\ i_{ds} - \omega_s\ \psi_{qs} + \frac{d}{dt}\psi_{ds} \quad (9)$$

$$v_{qs} = -R_s\ i_{qs} + \omega_s\ \psi_{ds} + \frac{d}{dt}\psi_{qs} \quad (10)$$

$$v_{dr} = -R_r\ i_{dr} - s\,\omega_s\ \psi_{qr} + \frac{d}{dt}\psi_{dr} \quad (11)$$

$$v_{qr} = -R_r\ i_{qr} + s\,\omega_s\ \psi_{dr} + \frac{d}{dt}\psi_{qr} \quad (12)$$

$$\Psi_{ds} = -L_{ss}\ i_{ds} - L_m\ i_{dr} \quad , \quad \Psi_{qs} = -L_{ss}\ i_{qs} - L_m\ i_{qr} \quad (13)$$

$$\Psi_{dr} = -L_{rr}\ i_{dr} - L_m\ i_{ds} \quad , \quad \Psi_{qr} = -L_{rr}\ i_{qr} - L_m\ i_{qs} \quad (14)$$

$$s = (\omega_s - \omega_r)/\omega_s \quad (15)$$

$$\frac{d\omega_r}{dt} = -\omega_s\frac{ds}{dt} \quad (16)$$

Where, $L_{ss} = L_s + L_m$, $L_{rr} = L_r + L_m$, L_s, L_r and L_m are the stator leakage, rotor leakage and mutual inductances, respectively. The previous model may be reduced by neglecting stator transients and is described as follows:

$$v_{ds} = -R_s\ i_{ds} + X'\ i_{qs} + e_d \quad (17)$$

$$v_{qs} = -R_s\ i_{qs} - X'\ i_{ds} + e_q \quad (18)$$

$$\frac{de_d}{dt} = -\frac{1}{T_0}\left(e_d + (X - X)i_{qs}\right) + s\,\omega_s\,e_q - \omega_s\frac{L_m}{L_{rr}}v_{qr} \quad (19)$$

$$\frac{de_q}{dt} = -\frac{1}{T_0}\left(e_q - (X - X)i_{ds}\right) - s\,\omega_s\,e_d + \omega_s\frac{L_m}{L_{rr}}v_{dr} \quad (20)$$

The components of the voltage behind the transient are $e_d = -\frac{\omega_s L_m}{L_{rr}}\psi_{qr}$ and $e_q = \frac{\omega_s L_m}{L_{rr}}\psi_{dr}$. The stator reactance $X = \omega_s L_{ss} = X_s + X_m$, and the stator transient reactance $X' = \omega_s (L_{ss} - L_m^2/L_{rr}) = X_s + (X_r\ X_m)/(X_r + X_m)$. The transient open circuit time constant is $T_o = L_{rr}/R_r = (L_r + L_m)/R_r$, and the electrical torque is $T_e = (i_{ds}i_{qr} - i_{qs}i_{dr})X_m/\omega_s$. Figure (1) shows d and q – axis equivalent circuit of DFIG.

ISBN: 978-988-19252-3-7
ISSN: 2078-0958 (Print); ISSN: 2078-0966 (Online)

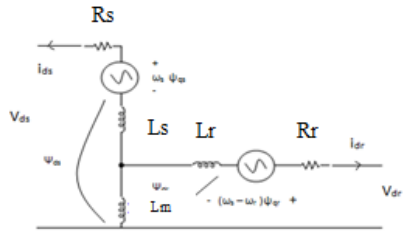

d – axis equivalent circuit of DFIG

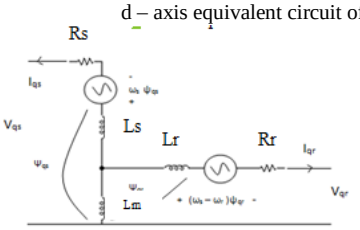

q – axis equivalent circuit of DFIG

Figure (1) d and q – axis equivalent circuit of DFIG.

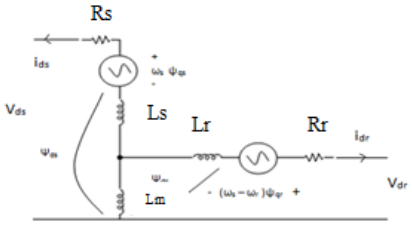

d – axis equivalent circuit of SCIG

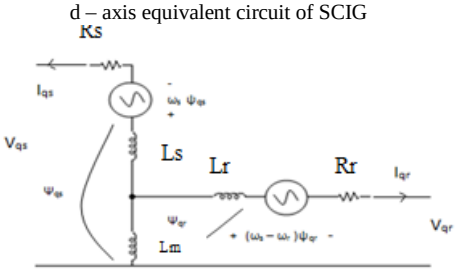

q – axis equivalent circuit of SCIG

Figure (2) d and q – axis equivalent circuit of FSIG

D. Dynamic Model of SCIG

In the SCIG the rotor is short circuited and so, the stator voltages are the Lm as the DFIG. In the SCIG there are capacitors to provide the induction generator magnetizing current and for compensation. Figure (2) d and q – axis equivalent circuit of FSIG.

E. The Pitch Controller Model

The pitch controller is used to adjust the tidal current turbine to achieve a high speed magnitude. This may be represented by a PI controller with a transfer function $K_{pt}+\frac{K_{it}}{s}$.

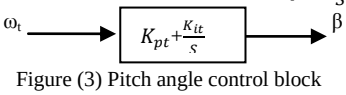

Figure (3) Pitch angle control block

$$\beta=(K_{pt}+\frac{K_{it}}{s})\omega_t \quad (21)$$

$$\frac{d\beta}{dt}=K_{pt}\frac{d\omega t}{dt}+K_{it}\omega_t \quad (22)$$

F. The Converter Model

A converter feeds or takes power from the rotor circuit and gives a variable speed (a partial scale power converter used). The rotor side of the DFIG is connected to the grid via a back to back converter. The converter at the side connected to the grid is called supply side converter (SSC) or grid side converter (GSC) while the converter connected to the rotor is the rotor side converter (RSC). The RSC operates in the stator flux reference frame. The direct axis component of the rotor current acts in the same way as the field current as in the synchronous generator and thus controls the reactive power change. The quadrature component of the rotor current is used to control the speed by controlling the torque and the active power change. Thus the RSC governs both the stator-side active and reactive powers independently. The GSC operates in the stator voltage reference frame. The *d*-axis current of the GSC controls the DC link voltage to a constant level, and the *q*-axis current is used for reactive power control. The GSC is used to supply or draw power from the grid according to the speed of the machine. If the speed is higher than synchronous speed it supplies power, otherwise it draws power from the grid but its main objective is to keep dc-link voltage constant regardless of the magnitude and direction of rotor power The back to back converter using a DC link is shown in Figure (4). The balanced power equation is given by [13, 14]:

$$P_r=P_q+P_{DC} \quad (23)$$

$$P_{DC}=v_{DC}i_{DC}=-Cv_{DC}\frac{dv_{DC}}{dt}, \quad P_g=v_{Dg}i_{Dg}+v_{Qg}i_{Qg} \quad (24)$$

$$Cv_{DC}\frac{dv_{DC}}{dt} = v_{Dg}i_{Dg}+v_{Qg}i_{Qg} - v_{dr}\ i_{dr} - v_{qr}\ i_{qr} \quad (25)$$

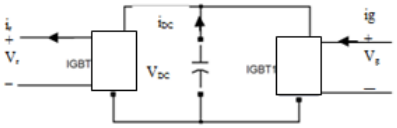

Figure (4) Back to back converter

G. Rotor Side Converter Controller Model

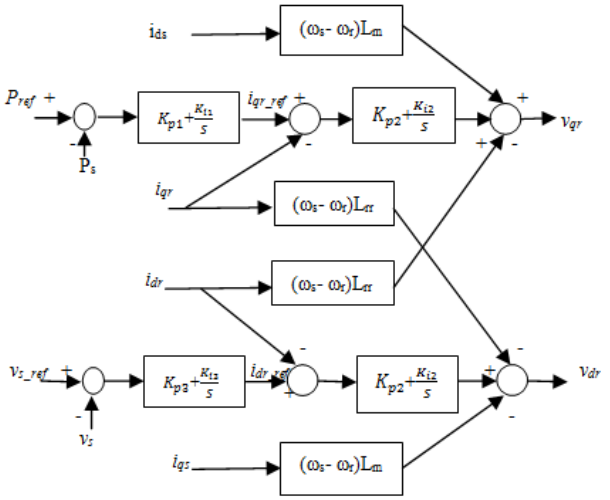

Figure (5) Generator side converter controller

The rotor side converter controller used here is represented by four states ($\dot{x}_1$, $\dot{x}_2$, $\dot{x}_3$ and $\dot{x}_4$), $\dot{x}_1$ is related to the difference between the generated power of the stator and the reference power that is required at a certain time, $\dot{x}_2$ is related to the difference between the quadrature axis generator rotor current and the reference current that is required at a certain time, $\dot{x}_3$ is related to the difference between the stator terminal voltage and the reference

ISBN: 978-988-19252-3-7
ISSN: 2078-0958 (Print); ISSN: 2078-0966 (Online)

voltage that is required at a certain time, and $\dot{x}_4$ is related to the difference between the direct axis generator rotor current and the reference current that is required at a certain time [13, 14]. Figure (5) shows the rotor side converter controller. This is described by equations (26-34).

$$\dot{x}_1 = P_{ref} - P_s \quad (26)$$
$$\dot{x}_1 = -K_{i1}/K_{p1} x_1 + 1/K_{p1}\, i_{qr\_ref} \quad (27)$$
$$\dot{x}_2 = i_{qr\_ref} - i_{qr} \quad (28)$$
$$\dot{x}_2 = K_{p1}\dot{x}_1 + K_{i1} x_1 - i_{qr} \quad (29)$$
$$\dot{x}_2 = -K_{i2}/K_{p2} x_2 + 1/K_{p2}\, v_{qr} - \omega_s L_m/K_{p2}\, i_{ds} - \omega_s L_{rr}/K_{p2} i_{dr} + (L_m/K_{p2})\, i_{ds}\omega_r + (L_{rr}/K_{p2}) i_{dr}\omega_r \quad (30)$$
$$\dot{x}_3 = v_{s\_ref} - v_s \quad (31)$$
$$\dot{x}_3 = -K_{i3}/K_{p3} x_3 + 1/K_{p3}\, i_{dr\_ref} \quad (32)$$
$$\dot{x}_4 = i_{dr\_ref} - i_{dr} \quad (33)$$
$$\dot{x}_4 = -K_{i2}/K_{p2} x_4 + 1/K_{p2}\, v_{dr} - \omega_s L_m/K_{p2}\, i_{qs} - \omega_s L_{rr}/K_{p2} i_{qr} + (L_m/K_{p2})\, i_{qs}\omega_r + (L_{rr}/K_{p2}) i_{qr}\omega_r \quad (34)$$

H. Grid Side Converter Controller Model

The grid side converter controller used here is represented by four states ($\dot{x}_5$, $\dot{x}_6$, $\dot{x}_7$ and $\dot{x}_8$), x_5 is related to the difference between the DC voltage and the reference DC voltage required at a certain time, x_6 related to the difference between the grid terminal voltage and the reference terminal voltage required at a certain time, x_6 is a combination of x_5 and direct axis grid current and x_8 is a combination of x_6 and quadrature axis grid current as shown in equations (35-40). Figure (6) shows the grid side converter controller.

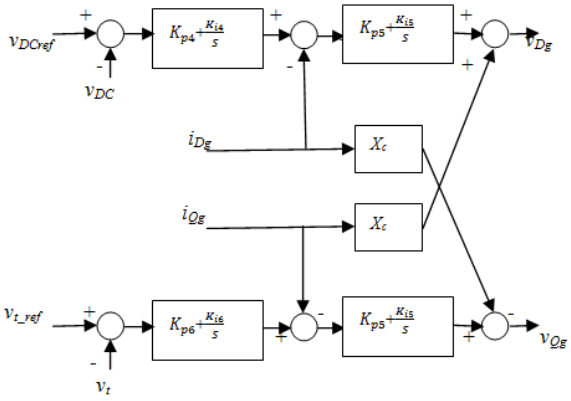

Figure (6) Grid side converter controller

$$\dot{x}_5 = v_{DC\_ref} - v_{DC} \quad (35)$$
$$\dot{x}_6 = K_{p4}\dot{x}_5 + K_{i4} x_5 - i_{Dg} \quad (36)$$
$$\dot{x}_7 = v_{t\_ref} - v_t \quad (37)$$
$$\dot{x}_8 = K_{p6}\dot{x}_7 + K_{i6} x_7 - i_{Qg} \quad (38)$$
$$v_{Dg} = K_{p5}\dot{x}_6 + K_{i5} x_6 + X_c i_{Qg} \quad (39)$$
$$v_{Qg} = K_{p5}\dot{x}_8 + K_{i5} x_8 - X_c i_{Dg} \quad (40)$$

III. Tidal Current Turbine Model Using DDPMSG

A. The Dynamic Modeling of The DDPMSG

The DDPMSG can be modeled as the following [3, 13]:

$$v_{ds} = -R_s \times i_{ds} - \omega_s \times \psi_{qs} + \frac{d}{dt}\psi_{ds} \quad (41)$$
$$v_{qs} = -R_s \times i_{qs} + \omega_s \times \psi_{ds} + \frac{d}{dt}\psi_{qs} \quad (42)$$

The flux linkages and the torque can be expressed as:

$$\Psi_{ds} = -L_d \times i_{ds} + \psi_f \quad (43)$$
$$\Psi_{qs} = -L_q \times i_{qs} \quad (44)$$
$$T_e = (3/2)p\, i_{qs}((L_d - L_q)\, i_{ds} + \psi_f) \quad (45)$$

L_d, and L_q are the direct and quadrature inductances of the stator. Ψ_f is the excitation field linkage, and p is the number of pair poles. Figure (7) shows the d-q axis component of the DDPMSG. In this paper for simplicity we will assume that $L_d = L_q = L_s$, and so the generator model can be rewritten in a state space representation as:

$$L_s \frac{d}{dt} i_{ds} = -v_{ds} - R_s \times i_{ds} + L_s \times \omega_s \times i_{qs} \quad (46)$$
$$L_s \frac{d}{dt} i_{qs} = -v_{qs} - R_s \times i_{qs} - L_s \times \omega_s \times i_{ds} + \omega \times \psi_f \quad (47)$$

The converters models used for the DFIG are the same converters that used for the DDPMSG keeping in mind that a full scale power converter is used.

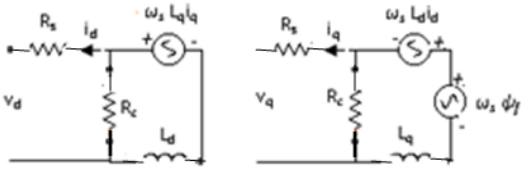

Figure (7) d-q axis component of PMSG

B. The Generator Side Converter Controller Model for DDPMSG

The generator side converter controller used here is represented by two states only (x_1, and x_2), x_1 related to the difference between the generated power and the reference power that required at a certain time and x_2 related to the difference between the direct axis generator current and the reference current that required at a certain time [13-15]. Figure (8) shows the generator side converter controller described by:

$$\dot{x}_1 = P_s - P_{ref} \quad (48)$$
$$\dot{x}_2 = i_{ds} - i_{ds\_ref} \quad (49)$$
$$v_{qs} = K_{p1}\dot{x}_1 + K_{i1} x_1 - L_s w i_{ds} \quad (50)$$
$$v_{ds} = K_{p2}\dot{x}_2 + K_{i2} x_2 + L_s w i_{qs} \quad (51)$$

Where: K_{p1}, K_{p2}, represent the proportional controller constants and K_{i1}, K_{i2} represent the integral controller constants for the generator side converter controller.

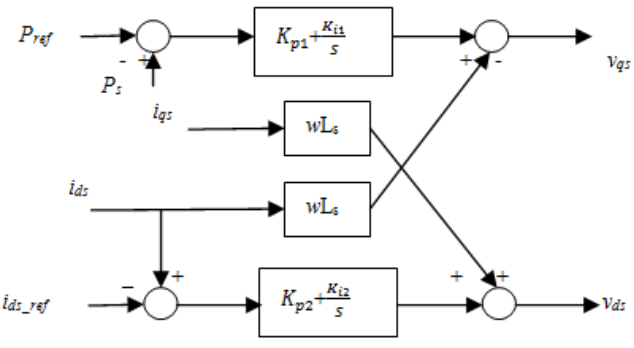

Figure (8) Generator side converter controller for DDPMSG

C. The Grid Side Converter Controller Model for DDPMSG

The grid side converter controller used here is represented by four states (x_3, x_4, x_5, x_6), x_3 related to the difference between the DC voltage and the reference DC voltage that required at a certain time, x_5 related to the difference between the terminal voltage and the reference terminal voltage that required at a certain time, x_4 is a combination of x_3 and direct axis grid current and x_6 is a combination of x_4

ISBN: 978-988-19252-3-7
ISSN: 2078-0958 (Print); ISSN: 2078-0966 (Online)

and quadrature axis grid current. Figure (9) shows the grid side converter controller.

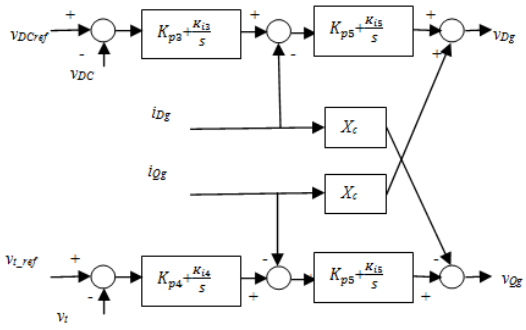

Figure (9) Grid side converter controller for DDPMSG

$$\dot{x}_3 = v_{sDC\_ref} - v_{DC} \quad (52)$$
$$\dot{x}_4 = K_{p3}\dot{x}_3 + K_{i3}x_3 - i_{Dq} \quad (53)$$
$$\dot{x}_5 = v_{t\_ref} - v_t \quad (54)$$
$$\dot{x}_6 = K_{p4}\dot{x}_4 + K_{i4}x_5 - i_{Qg} \quad (55)$$
$$v_{Dg} = K_{p5}\dot{x}_4 + K_{i5}x_4 + X_c i_{Qg} \quad (56)$$
$$v_{Qg} = K_{p5}\dot{x}_6 + K_{i5}x_6 - X_c i_{Dq} \quad (57)$$

Where: V_{DC} is the DC link voltage, i_{Dg}, i_{Qg} are the D and Q axis grid currents, v_{Dg}, v_{Qg} are the D and Q axis grid voltages, K_{p3}, K_{p4}, K_{p5} represent the proportional controller constants, X_c is the grid side smoothing reactance, and K_{i3}, K_{i4}, K_{i5} represent the integral controller constants for the grid side converter.

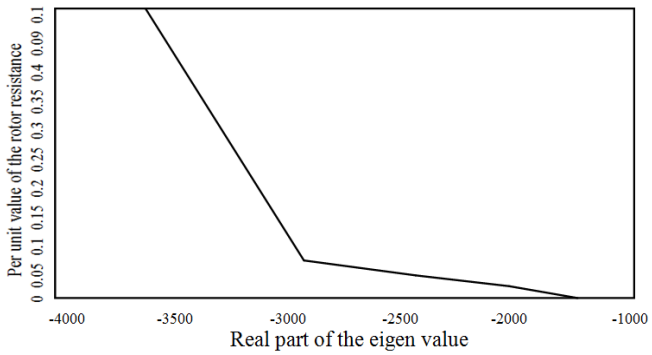

Figure (10) The relation between different values of the rotor resistance and the eigenvalues of the changed mode in case of DFIG.

IV. Validation of the Models

As the value of the resistance or inductance changes the stability degree will change. Figure (10) shows the relation between different values of the rotor resistance and the eigenvalues of the changed mode in case of DFIG. Figure (11) shows the relation between different values of the stator resistance and the eigenvalues of the changed mode in case of DDPMSG. Figure (12) shows the relation between different values of the rotor inductance and the eigenvalues of the changed mode in case of DFIG. Figure (13) shows the relation between different values of the stator inductance and the eigenvalues of the changed mode in case of DDPMSG. As the resistance value of the rotor increase, the stability degree will increase and as the inductance value increase as the stability will decrease because of increasing the delay time.

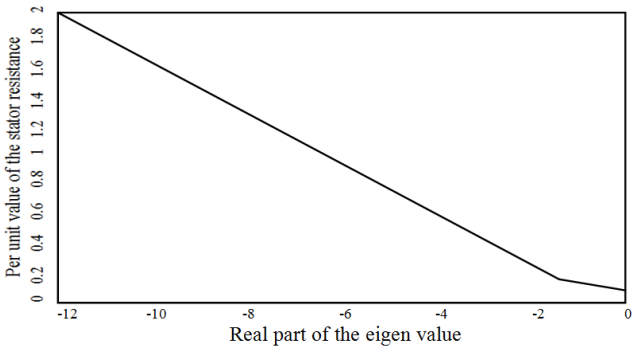

Figure (11) The relation between different values of the stator resistance and the eigenvalues of the changed mode in case of DDPMSG.

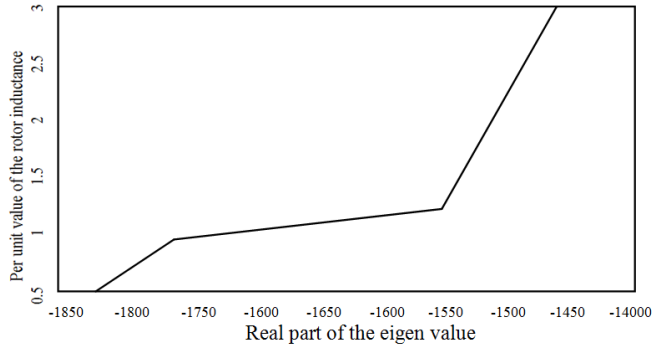

Figure (12) The relation between different values of the rotor inductance and the eigenvalues of the changed mode in case of DFIG.

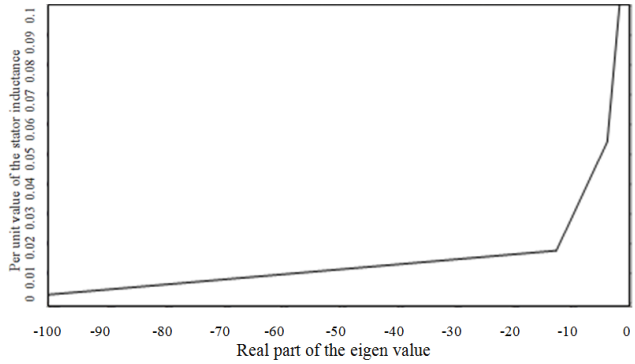

Figure (13) The relation between different values of the stator self inductance and the eigenvalues of the changed mode in case of DDPMSG.

V. Conclusion

The use of offshore wind and tidal current as a renewable source of energy is very effective as it relies on similar technologies. The overall dynamic system of the offshore and tidal current turbine based on three different types of generators for a single machine infinite bus system has been modeled. The converter used has been modelled. Different controller models are also discussed for different machines. The state space representation of the overall system is concluded. All models are validated using a common property of the machine for the validation (changing the degree of the system stability by changing of the value of the resistance and the inductance). If the resistance value of different generators increases, the stability degree will increase and if the inductance value of the machine increases, the stability degree will decrease. The tidal current energy is more predictable compared to offshore wind energy. It is beneficial to use a hybrid of offshore wind and tidal current turbine.

ISBN: 978-988-19252-3-7
ISSN: 2078-0958 (Print); ISSN: 2078-0966 (Online)

ACKNOWLEDGMENT

The first author would like to thank the Egyptian Government for supporting this work.

REFERENCES

[1] "Tidal Stream" Available online (January 2011), http://www.tidalstream.co.uk/html/background.html
[2] "Tidal Currents" Available online (April 2011), http://science.howstuffworks.com/environmental/earth/oceanography/ocean-current4.htm
[3] Hamed H. H. Aly, and M. E. El-Hawary "State of the Art for Tidal Currents Electrical Energy Resources", 24th Annual Canadian IEEE Conference on Electrical and Computer Engineering, Niagara Falls, Ontario, Canada, 2011.
[4] Hamed H. Aly, and M. E. El-Hawary "An Overview of Offshore Wind Electrical Energy Systems" 23rd Annual Canadian IEEE Conference on Electrical and Computer Engineering, Calgary, Alberta, Canada, May 2-5, 2010.
[5] Marcus V. A. Nunes, J. A. Peças Lopes, Hans Helmut, Ubiratan H. Bezerra, and Rogério G. "Influence of the Variable-Speed Wind Generators in Transient Stability Margin of the Conventional Generators Integrated in Electrical Grids" IEEE Transactions on Energy Conversion, 2004.
[6] J.G. Slootweg, H. Polinder and W.L. Kling"Dynamic Modeling of a Wind Turbine with Doubly Fed Induction Generator" IEEE Power Engineering Society Summer Meeting, 2001.
[7] Janaka B. Ekanayake, Lee Holdsworth, XueGuang Wu, and Nicholas Jenkins" Dynamic Modeling of Doubly Fed Induction Generator Wind Turbines" IEEE Transactions on Power Systems, Vol. 18, No. 2, May 2003.
[8] M.J.Khan, G. Bhuyan, A. Moshref, K. Morison, "An Assessment of Variable Characteristics of the Pacific Northwest Regions Wave and Tidal Current Power Resources, and their Interaction with Electricity Demand & Implications for Large Scale Development Scenarios for the Region," Tech. Rep. 17485-21-00 (Rep 3), Jan. 2008.
[9] Lucian Mihet-Popa, Frede Blaabjerg, and Ion Boldea," Wind Turbine Generator Modeling and Simulation Where Rotational Speed is the Controlled Variable" IEEE Transactions On Industry Applications, Vol. 58, No. 1, January/February 2004.
[10] Hamed H. H. Aly, M. E. El-Hawary "A Proposed Algorithms for Tidal in-Stream Speed Model" American Journal of Energy Engineering. Vol. 1, No. 1, 2013, pp. 1-10.
[11] Hamed H. H. Aly, M. E. El-Hawary. The Current Status of Wind and Tidal in-Stream Electric Energy Resources, American Journal of Electrical Power and Energy Systems. Vol. 2, No. 2, 2013, pp. 23-40.
[12] Yazhou Lei, Alan Mullane, Gordon Lightbody, and Robert Yacamini "Modeling of the Wind Turbine with a Doubly Fed Induction Generator for Grid Integration Studies" IEEE Transaction on Energy Conversion, Vol. 28, No. 1, March 2006.
[13] F. Wu, X.-P. Zhang, and P. Ju "Small signal stability analysis and control of the wind turbine with the direct-drive permanent magnet generator integrated to the grid" Journal of Electric Power and Engineering Research, 2009.
[14] F. Wu, X.-P. Zhang, and P. Ju "Small signal stability analysis and optimal control of a wind turbine with doubly fed induction generator" IET Journal of Generation, Transmission and Distribution, 2007.
[15] Hamed H. Aly "Forecasting, Modeling, and Control of Tidal currents Electrical Energy Systems"PhD thesis, Halifax, Canada. 2012.

ISBN: 978-988-19252-3-7
ISSN: 2078-0958 (Print); ISSN: 2078-0966 (Online)